Protein delivery by porous cationic maltodextrin-based nanoparticles into nasal mucosal cells: Comparison with cationic or anionic nanoparticles

Minh Quan Lê, Rodolphe Carpentier, Isabelle Lantier, Céline Ducournau, François Fasquelle, Isabelle Dimier-Poisson, Didier Betbeder

▶ **To cite this version:**

Minh Quan Lê, Rodolphe Carpentier, Isabelle Lantier, Céline Ducournau, François Fasquelle, et al.. Protein delivery by porous cationic maltodextrin-based nanoparticles into nasal mucosal cells: Comparison with cationic or anionic nanoparticles. International Journal of Pharmaceutics: X, 2019, 1, 7 p. 10.1016/j.ijpx.2018.100001 . hal-02974070

HAL Id: hal-02974070
https://hal.inrae.fr/hal-02974070v1

Submitted on 21 Oct 2020

HAL is a multi-disciplinary open access archive for the deposit and dissemination of scientific research documents, whether they are published or not. The documents may come from teaching and research institutions in France or abroad, or from public or private research centers.

L'archive ouverte pluridisciplinaire **HAL**, est destinée au dépôt et à la diffusion de documents scientifiques de niveau recherche, publiés ou non, émanant des établissements d'enseignement et de recherche français ou étrangers, des laboratoires publics ou privés.

Distributed under a Creative Commons Attribution - NonCommercial - NoDerivatives 4.0 International License

International Journal of Pharmaceutics: X 1 (2019) 100001

Contents lists available at ScienceDirect

International Journal of Pharmaceutics: X

journal homepage: www.journals.elsevier.com/international-journal-of-pharmaceutics-x

Protein delivery by porous cationic maltodextrin-based nanoparticles into nasal mucosal cells: Comparison with cationic or anionic nanoparticles

Minh Quan Lê[a,b,c], Rodolphe Carpentier[a,b,c,*], Isabelle Lantier[d], Céline Ducournau[e], François Fasquelle[a,b,c], Isabelle Dimier-Poisson[e], Didier Betbeder[a,b,c,f]

[a] Inserm, LIRIC – UMR 995, F-59 000 Lille, France
[b] Univ Lille, LIRIC – UMR 995, F-59 045 Lille, France
[c] CHRU de Lille, LIRIC – UMR 995, F-59 000 Lille, France
[d] INRA – Université de Tours, UMR1282, F-37380 Nouzilly, France
[e] Université de Tours – INRA, UMR1282, F-37000 Tours, France
[f] Université d'Artois, 62300 Lens, France

ARTICLE INFO

Keywords:
Nanoparticles
Nasal
Vaccine
Protein delivery

ABSTRACT

Different types of biodegradable nanoparticles (NPs) have been studied as delivery systems for proteins into nasal mucosal cells, especially for vaccine applications. Such a nanocarrier must have the ability to be loaded with proteins and to transport this payload into mucosal cells. However, comparative data on nanoparticles' capacity for protein loading, efficiency of subsequent endocytosis and the quantity of nanocarriers used are either lacking or contradictory, making comparisons and the choice of a best candidate difficult. Here we compared 5 types of nanoparticles with different surface charge (anionic or cationic) and various inner compositions as potential vectors: the NPL (cationic maltodextrin NP with an anionic lipid core), cationic and anionic PLGA (Poly Lactic co-Glycolic Acid) NP, and cationic and anionic liposomes. We first quantified the protein association efficiency and NPL associated the largest amount of ovalbumin, used as a model protein. *In vitro*, the delivery of fluorescently-labeled ovalbumin into mucosal cells (airway epithelial cells, dendritic cells and macrophages) was assessed by flow cytometry and revealed that the NPL delivered protein to the greatest extent in all 3 different cell lines. Taken together, these data underlined the potential of the porous and cationic maltodextrin-based NPL as efficient protein delivery systems to mucosal cells.

1. Introduction

Nasal vaccination is an attractive strategy for the induction of mucosal and systemic immunity (Ogra et al., 2001; Zaman et al., 2013). Indeed, most pathogenic infections start at a mucosal surface and the induction of both local and distal mucosal immunity offers the possibility of neutralizing them at their point of entry. However, despite this clear advantage, as well as the practicality of needle-free administration, intranasal vaccination remains challenging owing largely to inefficient uptake and rapid clearance of the antigen.

Nanoparticles (NPs) have been tested as delivery systems for nasal vaccines and shown to improve the delivery of antigens to immune cells while limiting their mucosal clearance. Other advantages include their ability to protect antigens against enzymatic degradation and their ability to transport antigens across the mucous barrier (Bernocchi et al., 2017; Zhao et al., 2014). However, while many nanoparticulate delivery systems are described, no direct comparison between available types has so far been published, making it difficult to choose the ideal nanocarrier for this application.

Natural and synthetic biodegradable materials are generally used as components of nanoparticles. Polyester derivatives such as poly lactic-co-glycolic acid (PLGA), lipid-based nanoparticles such as liposomes, and polysaccharides such as chitosan, starch, alginate or dextran are the main candidates under evaluation (Bernocchi et al., 2017; Marasini et al., 2017). Maltodextrin-based nanoparticles (NPL) have been studied as delivery systems of antigens and drugs administered via the nasal route (Jallouli et al., 2007). These NP are made from cationic maltodextrin with an anionic phospholipid core. NPL can deliver antigens to the mucosal cells (Dombu et al., 2012). After intranasal administration of a NPL-based vaccine, an immune protection was observed after an oral challenge (Dimier-Poisson et al., 2015; Ducournau et al., 2017). NPL also increase the nasal residence time of proteins

* Corresponding author at: LIRIC – UMR995, Faculty of Medicine, Research Building, Group of Nanomedicine, Place de Verdun, 59045 Lille Cedex, France.
E-mail address: rodolphe.carpentier@univ-lille.fr (R. Carpentier).

https://doi.org/10.1016/j.ijpx.2018.100001
Received 2 July 2018; Received in revised form 29 November 2018; Accepted 6 December 2018
Available online 10 December 2018
2590-1567/ © 2018 The Author(s). Published by Elsevier B.V. This is an open access article under the CC BY-NC-ND license (http://creativecommons.org/licenses/BY-NC-ND/4.0/).

(Bernocchi et al., 2016). These studies strongly support the potential for NPL to be an excellent vaccine delivery system. PLGA is composed of two polymers: lactic acid and glycolic acid, linked by ester bonds easily metabolized by the body and auto-degradable. PLGA has been approved by the American Food and Drug Administration and European Medicine Agency (EMA) for human applications (Danhier et al., 2012) and it has been demonstrated that PLGA nanoparticles (PLGA NPs) are of interest for vaccines (Clawson et al., 2010; Diwan et al., 2003; Prasad et al., 2011; Solbrig et al., 2007; Thomas et al., 2011). Liposomes are spherical, self-closed structures consisting of one or several phospholipid bilayers enclosing an aqueous phase (Torchilin, 2005). Due to their lipid structure, they are bioavailable and able to entrap both hydrophilic and hydrophobic drugs – in addition, liposomes could have an adjuvant effect (De Serrano and Burkhart, 2017).

In order to compare different antigen delivery systems, different properties such as antigen loading capacity and cell delivery must be evaluated (Oh and Park, 2014). In this study, we compared the loading and delivery of antigens using three types of airway mucosal cells (airway epithelial cells, macrophages and dendritic cells). The study was performed on NPL (cationic on their surface and anionic in their porous core), on anionic and cationic PLGA and on anionic and cationic liposomes.

2. Material and methods

2.1. Materials

Maltodextrin was purchased from Roquette (France) while DPPG (1,2-dipalmitoyl-snglycero-3-phosphatidylglycerol) and DPPC (1,2-dipalmitoyl-sn-glycero-3-phosphocholine) were from Lipoid (Germany). Cell culture media (RPMI 1640 and IMDM), fetal calf serum (FCS), non-essential amino acids, trypsin, L-glutamine, phosphate buffered saline (PBS), NaOH, ethanol, DAPI (4,6-diamidino-2-phenylindole), DiI (1,10-dioctadecyl-3,3,30,30-tetramethylene) and Micro BCA Protein Assay Kit were purchased from ThermoFisher Scientific (France). PLGA (50:50, Acid copolymer: Resomer RG503H) was from Evonik (Germany). Epichlorhydrin (1-chloro-2,3-epoxypropane), GTMA (glycidyl-trimethyl-ammonium chloride), $NaBH_4$, chitosan, PD-10 Sephadex G25 desalting column, ovalbumin (OVA) and Fluorescein-5-isothiocyanate (FITC) were all purchased from Sigma-Aldrich (France).

The human muco-epidermoid bronchiolar carcinoma cell line NCI-H292 (hereafter H292) was supplied by Dr J.M. Lo-Guidice (University of Lille, France). The human monocytic cell line THP-1 was donated by Dr. F. Nesslany (Pasteur Institute of Lille, France). The CD4− CD8α+ CD205+ CD11b− murine spleen dendritic cell line SRDC line was obtained from Pr. I. Dimier-Poisson (University François-Rabelais of Tours, France) (Ruiz et al., 2005).

2.2. Cell culture

The H292 and THP-1 cells were maintained in RPMI supplemented with 10% heat-inactivated fetal calf serum (FCS), 100 U/mL Penicillin, 100 mg/mL streptomycin and 2 mM L-glutamine at 37 °C in humidified 5% CO_2 atmosphere. SRDC were cultured in IMDM supplemented with 5% heat-inactivated FCS, 100 U/mL Penicillin, 100 mg/mL streptomycin and 2 mM L-glutamine at 37 °C in humidified 5% CO_2 atmosphere. Cells were seeded 3 days before treatment at a density of 5×10^5 cells per well in 6-well plates. The differentiation of THP-1 into a macrophage-like, adherent phenotype was performed by adding 10 ng/ml to the culture media for 24 h.

2.3. Nanoparticles synthesis

2.3.1. NPL synthesis

NPL were prepared as described previously (Le et al., 2018; Paillard et al., 2010). A batch of 100 g of maltodextrin was dissolved in 2 N sodium hydroxide with magnetic stirring at room temperature. The mixture was reticulated and cationised overnight using epichlorhydrin (4.72 ml) and GTMA (31.18 g) to obtain hydrogels that were neutralized with acetic acid and sheared using a high pressure homogenizer (LM20, Microfluidics, France) with 3 cycles of 400 bars. The size of the nanoparticles thus obtained were determined by DLS (see below) and purified against ultrapure water by tangential flow ultra-filtration (AKTA flux 6, GE Healthcare, France) using a 750 kDa membrane (GE Healthcare, France). The absence of salts and maltodextrin fragments were confirmed by silver nitrate assay and DLS, respectively. The resulting porous, cationic maltodextrin nanoparticles (NP+) were post-loaded with 70% (w/w) DPPG above the gel-to-liquid phase transition temperature to produce NPL.

2.3.2. Cationic and anionic PLGA NPs

Anionic PLGA NPs were produced by nanoprecipitation at room temperature (Chang et al., 2009). The PLGA polymer was dissolved at 10 mg/mL in an acetone/ethanol mixture (85:15) composing the organic phase. Dissolution was performed for 5 min under stirring at 150 rpm. Dissolved PLGA was then injected into 10 ml of ultrapure water (aqueous phase) under stirring at 150 rpm. No surfactant was added at any step of the synthesis. Residual organic solvents were eliminated under vacuum evaporation for 5 min at 27 °C. For cationic PLGA NP (Le et al., 2018), the dissolved PLGA was injected into ultrapure water containing 10% chitosan (w/w of PLGA) (aqueous phase) under stirring at 150 rpm. A chitosan stock solution was prepared by dissolving 10 mg of chitosan in 1 ml of water containing 5% acid acetic (v/v).

2.3.3. Cationic and anionic liposomes

Liposomes were prepared as previously described (Le et al., 2018). For anionic liposomes, 35 mg of lipid (DPPC 80% and DPPG 20%) was dissolved in 2 ml of ethanol. Dissolution was performed for 5 min under stirring at 150 rpm. Dissolved lipids were then injected into 10 ml of ultrapure water (aqueous phase) at 80 °C under stirring at 150 rpm.

For cationic liposomes, 35 mg of DPPC dissolved in ethanol was injected into ultrapure water (aqueous phase) at 80 °C under stirring at 150 rpm, followed by the addition of 10% chitosan (w/w of lipid) at 80 °C. A chitosan stock solution was prepared by dissolving 10 mg of chitosan in 1 ml of water containing 5% acid acetic (v/v). No surfactant was added at any step of the synthesis. Residual organic solvents were eliminated under vacuum evaporation for 5 min at 27 °C.

2.4. Characterization of nanoparticles and formulations

The size (hydrodynamic diameter in Z-average) of nanoparticles and formulations was measured by dynamic light scattering in pure water. The zeta potentials were measured by electrophoretic mobility in pure water. Measurements were carried out in triplicate using a zetasizer nanoZS (Malvern Instruments, France) with a particle concentration of 100 µg/ml.

2.5. Labeling of ovalbumin

Ovalbumin (OVA) was labeled with FITC according to a previously described protocol (Dimier-Poisson et al., 2015). Briefly, FITC was added to proteins solubilized in 0.1 M bicarbonate buffer (pH 9.5) at a ratio of 1/10 (w/w), and the solution was stirred for 6 h in the dark at room temperature. Gel permeation chromatography on a PD-10 Sephadex G25 desalting column (Sigma-Aldrich, France) was used to separate any free fluorescein from protein-associated dye. The fluorescence of the chromatographic fractions was analyzed by fluorometry using a Fluoroskan Ascent (ThermoScientific, France). Under these conditions, the fluorescence was thus due exclusively to OVA-FITC. The labeled protein was kept in the dark at 4 °C before use.

2.6. Post-loading of protein onto nanoparticles

The loading of different nanoparticles with OVA was performed by mixing both components in solution at room temperature for 1 h at an OVA/NP ratio of 1/10 or 3/10 (w/w).

2.7. Characterization of the association of protein with NP

The OVA protein association to the 5 types of NP was evaluated using native polyacrylamide gel electrophoresis (native PAGE). Formulations were supplemented with a non-denaturing buffer (Tris–HCL 125 mm (pH 6.8), 10% glycerol and 0.06% bromophenol blue) and run on a 10% acrylamide-bisacrylamide gels for 1.5 h at 120 V then stained by the silver nitrate method. Gels were scanned and quantified using the ImageJ software, setting the 0% of association over the OVA alone input. Under these conditions, non-associated protein enters the gel while NP-associated protein does not.

2.8. Protein delivery by nanoparticles in cells

Cells were plated for 3 days in 6-well plates as described in Section 2.2 and treated for different times (0.5, 2, 6, and 24 h) with 1 µg of OVA-FITC either in a free state, or associated with 10 µg of nanoparticles (1/10 w/w ratio). The cells were washed with PBS and collected using trypsin, immediately inhibited by the addition of serum. The cells were then centrifuged and resuspended with PBS just prior to analysis by flow cytometry with a BD Accuri™ C6 CFlow Sampler flow cytometer (BD Bioscience, USA). The cells were selected related to their size and complexity and the mean fluorescence intensities corresponding to the amount of particles taken up or adsorbed to the cells were reported.

3. Results

3.1. Fabrication and protein association characterization

The five types of nanoparticles were synthesized and their size and zeta potential were characterized (Figs. 1 and 2). The 2 anionic nanoparticles prepared: anionic PLGA NP (PLGA(−)) and anionic liposome (Lipo(−)), exhibited a zeta potential of −23 and −52 mV, respectively. Cationic nanoparticles were also prepared by covering nanoparticles with chitosan. PLGA(+) had a zeta potential of +38 mV while Lipo(+) had a zeta potential of +25 mV. NPL are porous nanoparticles with a cationic surface and an anionic lipid core: they therefore appeared as cationic nanoparticles with a zeta potential of +45 mV. The nanoparticles all possessed a Z-average size ranging from 57 to 161 nm. In addition, all these nanoparticles were spherical in shape (Carpentier et al., 2018; Dimier-Poisson et al., 2015; Gradauer et al., 2012; Movva Snehalatha, 2008; Sanna et al., 2012).

The OVA appeared as a 6 nm-protein with a negative surface charge of −15 mV. The association of OVA to NPL did not change the nanoparticles' size and only a slight decrease (−8 mV) of the zeta potential was observed, meaning that proteins were associated inside these porous nanoparticles. The formulations OVA/PLGA(+) and OVA/PLGA(−) showed a slight decrease of their respective surface charges (+30 mV and −18 mV) and both PLGA formulations retained their size. Finally, the OVA formulations with the liposomes increased their size by around 20 nm and drastically modified the zeta potential: 0 mV for Lipo(+) and −10 mV for Lipo(−).

This suggested an association of OVA with the 5 types of nanoparticles and this was confirmed by native PAGE (Table 1). At a mass ratio OVA/NP of 1/10, nanoparticles with a positive surface charge associated 90% of the OVA, and even 100% for NPL. By contrast anionic nanoparticles associated only 10% (Lipo(−)) to 50% (PLGA(−)) of the OVA. To highlight differences in the protein loading capacity of the nanoparticles, particularly the cationic NP, a mass ratio OVA/NP of 3/10 was also examined. NPL still associated 100% of the OVA. The loading reached 70% for PLGA(+) but fell to only 10% for Lipo(+). Regarding the anionic nanoparticles, the loading of OVA with the mass ratio 3/10 was null for Lipo(−) and 20% for PLGA(−).

Hence, the ratio of 1/10 (w/w) of the OVA/NP was used in the following formulation experiments.

3.2. Comparison of the protein delivery by nanoparticles in H292 airway epithelial cells

Epithelial tissue covers the outside of the body and lines organs and cavities. The first barriers that nanoparticles face once nasally instilled are primarily the airway epithelial cells and some specialised cells such as microfold (M) cells (Rivera et al., 2016; Weitnauer et al., 2016). We evaluated the delivery of protein by the 5 types of nanoparticles into H292 airway epithelial cells using flow cytometry for 24 h (Kurakula et al., 2015). The endocytosis of OVA alone increased for 2 h then constantly decreased until 24 h, where intracellular OVA was no longer detectable. Nevertheless, even the maximum amount of endocytosed OVA was still low. OVA delivery by NPL was rapid and 14 times more efficient than protein alone at 2 h, whereupon the delivery reached a steady-state. The kinetics of protein delivery by PLGA(+) was comparable to those of the PLGA(−) until 6 h then a decrease was observed. PLGA(−) showed a similar profile to NPL (an initial and rapid protein delivery within 2 h followed by a steady-state), but were only 3 times more efficient than OVA alone. The delivery of OVA by Lipo(+) was firstly as efficient and quick as PLGA NP then decreased after 2 h. With Lipo(−), the OVA delivery increased during the first 2 h, being roughly

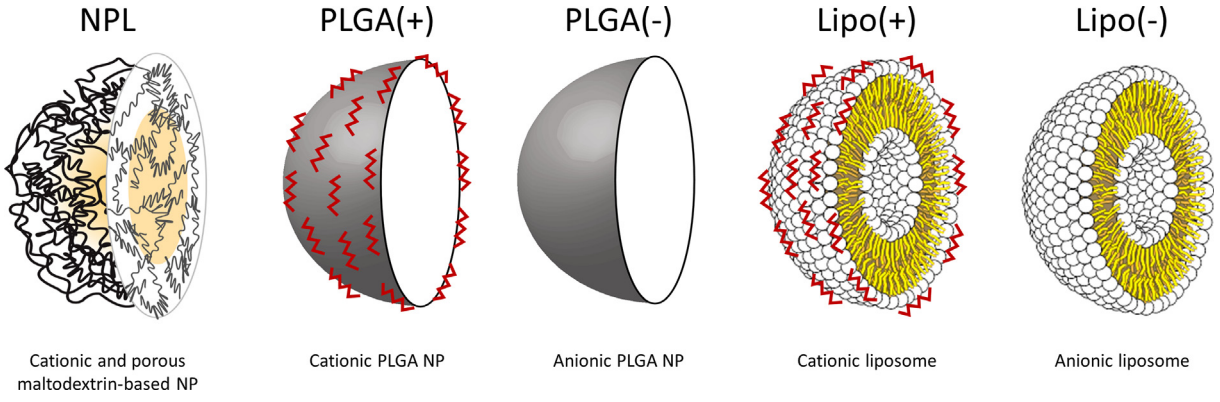

Fig. 1. Representation of the 5 types of nanoparticles. Cross sectional view showing the surface and the core of the nanoparticles. NPL: cationic maltodextrin-based porous nanoparticle with anionic lipid core, PLGA(+): cationic (chitosan-coated) PLGA nanoparticle, PLGA(−): anionic PLGA nanoparticle, Lipo(+): cationic (chitosan-coated) liposome, Lipo(−): anionic liposome.

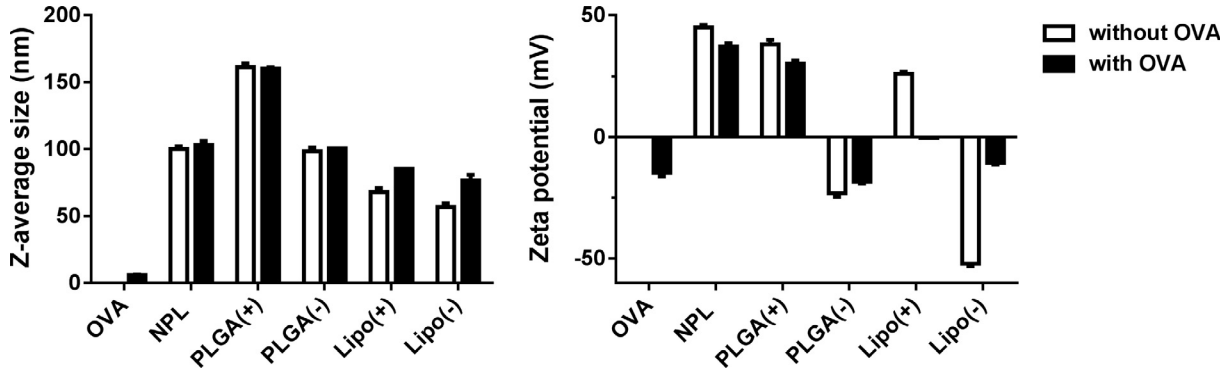

Fig. 2. Size and zeta potential of the 5 types of nanoparticles and their formulations with OVA. The nanoparticles' size (left) and the zeta potential (right) of ovalbumin (OVA), the 5 types of nanoparticles and their formulations with OVA at a mass ratio of 1/10 (OVA/NP), were measured by dynamic light scattering and electrophoretic mobility, respectively. The graphs represent the mean +/− SD of three independent measurements. NPL: cationic maltodextrin-based porous nanoparticle with anionic lipid core, PLGA(+): cationic (chitosan-coated) PLGA nanoparticle, PLGA(−): anionic PLGA nanoparticle, Lipo(+): cationic (chitosan-coated) liposome, Lipo(−): anionic liposome.

Table 1
Loading efficacy of OVA with the 5 types of nanoparticles. Native PAGE were run with the OVA/NP formulations at 1/10 and 3/10 mass ratios and non-associated proteins were determined by gel densitometry. The percentages of association with the NP were calculated by comparison with the 100% OVA reading and are reported in the table. NPL: cationic maltodextrin-based porous nanoparticle with anionic lipid core, PLGA(+): cationic (chitosan-coated) PLGA nanoparticle, PLGA(−): anionic PLGA nanoparticle, Lipo(+): cationic (chitosan-coated) liposome, Lipo(−): anionic liposome.

Formulations	OVA/NP ratio (w/w)	
	1/10	3/10
OVA/NPL	100%	100%
OVA/PLGA(+)	90%	70%
OVA/PLGA(−)	50%	20%
OVA/Lipo(+)	90%	10%
OVA/Lipo(−)	10%	0%

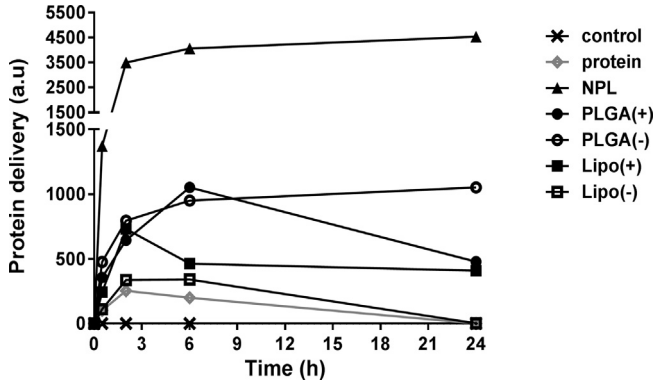

Fig. 3. Protein delivery by the 5 types of nanoparticles in H292 airway epithelial cells. Ovalbumin (OVA) was labeled with fluorescein and cells were treated with OVA (protein, grey line) or OVA/NP formulations (1/10 w/w ratio). The kinetics of protein delivery by the 5 types of nanoparticles (or the protein endocytosis for non-formulated OVA) were evaluated by flow cytometry. Representative graph of three independent experiments. NPL: cationic maltodextrin-based porous nanoparticle with anionic lipid core, PLGA(+): cationic (chitosan-coated) PLGA nanoparticle, PLGA(−): anionic PLGA nanoparticle, Lipo(+): cationic (chitosan-coated) liposome, Lipo(−): anionic liposome, Control: untreated cells.

half as efficient as Lipo(+), then decreased to reach a similar value to the OVA alone. Finally, at 24 h, NPL had delivered OVA 10 times more efficiently than PLGA(+) and Lipo(+) and 4 times more than PLGA(−) while OVA alone or associated with Lipo(−) was not detectable (Fig. 3). Together, all the 5 types of nanoparticles delivered OVA into the cells but major differences in the kinetics of the delivery and in its efficiency were highlighted.

3.3. Comparison of the protein delivery by nanoparticles in SRDCs dendritic cells

Nasal- or nasopharynx-associated lymphoid tissue (NALT) represents the immune system of nasal mucosa and is a part of mucosa-associated lymphoid tissue. The NALT is specifically enriched in dendritic cells (DCs) (Azizi et al., 2010; Bankvall et al., 2018; Boyaka, 2017) that pick up the antigens from M-cells, or directly through the epithelial layer, for subsequent antigen presentation and immune response triggering (Fujkuyama et al., 2012). OVA alone was slowly and weakly endocytosed for 2 h before reaching a steady-state. By comparison, the 5 types of nanoparticles showed a rapid initial delivery of OVA into DC during the first 30 min. At 30 min, NPL displayed the most efficient protein delivery (235 times more than OVA) followed by Lipo(−) (×90), Lipo(+) (×60), PLGA(−) (×20) then PLGA(+) (×15). After 30 min, the 5 types of nanoparticles behaved differently: NPL and Lipo(−) reached a steady-state, while protein kept being delivered until 6 h for the other NP. At 24 h, NPL had delivered OVA 16 times more efficiently than non-associated protein, while the 4 other types of nanoparticle showed an increase limited to ×4 for PLGA(−) to ×7 for PLGA(+), while liposomes had only intermediary values (Fig. 4). This comparison meant that NPL was once more the most efficient nanoparticle-based protein delivery system into DC.

3.4. Comparison of the protein delivery by nanoparticles into THP-1 macrophages

As the presence of macrophages in the airways has been documented (Juliusson et al., 1991), we examined the ability of the 5 types of nanoparticles to deliver proteins into macrophages. Compared to the other cell types in this study, the kinetics of protein delivery (and endocytosis of OVA alone) were more homogenous in THP-1, though the rate slightly decreased after 6 h. After 30 min, the delivery of OVA by the 5 types of nanoparticles was equivalent to the endocytosis of OVA alone. After 2 h, differences appeared and remained constant until 24 h, when NPL were 3 times more efficient than OVA alone while the 4 other types of nanoparticles were only by 1.5–1.7 times better at delivering OVA into THP-1 (Fig. 5). This again demonstrated that NPL was the most efficient nanoparticle in delivering OVA into macrophages.

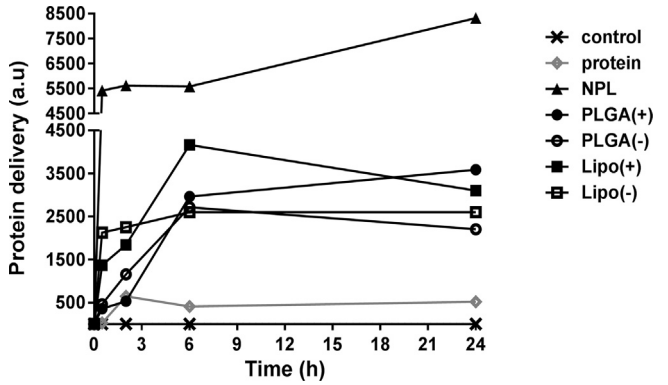

Fig. 4. Protein delivery by the 5 types of nanoparticles in SRDC dendritic cells. Ovalbumin (OVA) was labeled with fluorescein and cells were treated with OVA (protein, grey line) or OVA/NP formulations (1/10 w/w ratio). The kinetics of protein delivery by the 5 types of nanoparticles (or the protein endocytosis for non-formulated OVA) were evaluated by flow cytometry. Representative graph of three independent experiments. NPL: cationic maltodextrin-based porous nanoparticle with anionic lipid core, PLGA(+): cationic (chitosan-coated) PLGA nanoparticle, PLGA(−): anionic PLGA nanoparticle, Lipo(+): cationic (chitosan-coated) liposome, Lipo(−): anionic liposome, Control : untreated cells.

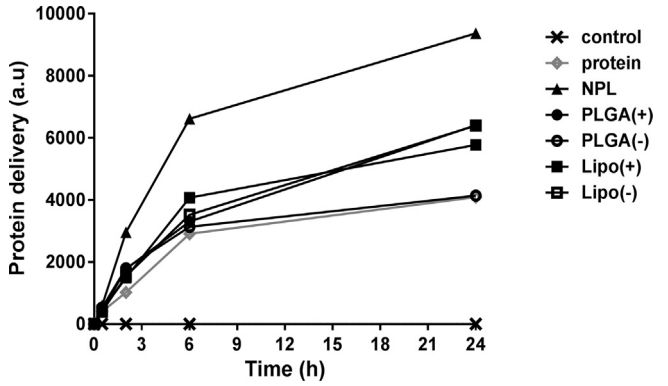

Fig. 5. Protein delivery by the 5 types of nanoparticles into THP-1-derived macrophages. Ovalbumin (OVA) was labeled with fluorescein and cells were treated with OVA (protein, grey line) or OVA/NP formulations (1/10 w/w ratio). The kinetics of protein delivery by the 5 types of nanoparticles (or the protein endocytosis for non-formulated OVA) were evaluated by flow cytometry. Representative graph of three independent experiments. NPL: cationic maltodextrin-based porous nanoparticle with anionic lipid core, PLGA(+): cationic (chitosan-coated) PLGA nanoparticle, PLGA(−): anionic PLGA nanoparticle, Lipo(+): cationic (chitosan-coated) liposome, Lipo(−): anionic liposome, Control: untreated cells.

4. Discussion

The vast majority of pathogens invade at the mucosal surfaces in the body and mucosal vaccination is a promising strategy for the induction of protective, mucosal-specific immunity. The nasal route is advantageous because of the presence of the relatively accessible nasal associated lymphoid tissue (NALT). However, nasally administered antigens are quickly cleared from nasal mucosal surfaces and delivery systems that protect antigens from this rapid clearance are needed (Csaba et al., 2009; Zaman et al., 2013). The challenge is developing a delivery system that protects antigens from clearance and degradation, and improves their delivery to cells (Pachioni-Vasconcelos Jde et al., 2016). An increasing number of nanocarriers have been used in nasal vaccine applications such as micelles, liposomes, polysaccharide nanoparticles and PLGA nanoparticles (Marasini et al., 2017). Nonetheless, no comparison of the vaccine efficiency of these nanocarriers has yet been published.

We previously compared the *in vivo* nasal residence time and the endocytosis of the 5 types of nanoparticles: the porous cationic maltodextrin-based NPL, the cationic or anionic PLGA NP, the cationic or anionic liposomes, and showed that NPL had the longest residence time and were the most efficiently endocytosed by the 3 cell lines used in this study (Le et al., 2018). Here we compared the antigen loading and the cellular delivery efficacy of these 5 types of nanoparticles, using OVA as a model protein.

The original preparation method of NPL has been described elsewhere (Bernocchi et al., 2016; Dimier-Poisson et al., 2015). In our comparative study, we here selected the nanoprecipitation method to produce PLGA NP and the solvent diffusion/injection method for the liposomes. These methods have the advantage of producing pure particles in water without the need for other components or filtration/purification steps. Moreover, the produced particles had a narrow size range ((Batzri and Korn, 1973; Le Broc-Ryckewaert et al., 2013; Le et al., 2018; Patil and Jadhav, 2014) and Table 1) compatible with our comparison.

Many studies have evaluated the protein loading efficiency of nanocarriers as a priority condition for their use as a vaccine delivery system. Accordingly, we compared the protein loading efficacy of the 5 types of NP. We chose ovalbumin as a model protein for our study. Indeed, OVA is negatively charged at physiological pH and contains hydrophobic regions. The 5 types of nanoparticles are hydrophobic and 3 of them possessed a positive surface charge. The interactions between OVA and the cationic nanoparticles are the result of ionic and non-ionic interactions. Among the 5 types of nanoparticles, only the NPL showed 100% of protein loading at mass ratios of 1/10 and 3/10 (OVA/NP). Neither PLGA NP nor liposomes reached this level of protein loading (Colletier et al., 2002; Lee et al., 2011; Yang and Luo, 2017) (Fig. 1 and Table 1). This is likely due to the structure of the nanoparticles: NPL are porous and their cationic surface available for interaction with protein is larger than non-porous nanoparticles like PLGA NP and liposomes, where protein interactions are limited to the nanoparticles' surface. With liposomes, we observed an increase of the size and a decrease of the zeta potential that approached the zeta potential of the free protein, clearly demonstrating an association of OVA with these NPs at their surface (Fig. 2). This association reached saturation since increasing the OVA/NP ratio led to a decrease of efficiency (Table 1). To increase the protein loading, OVA should have been entrapped in the liposomes as previously described but the loading efficiency remains low (Colletier et al., 2002; Watson et al., 2012) and efforts to increase the protein loading efficiency lead to size heterogeneity incompatible with pharmaceutical applications (Xu et al., 2011). With PLGA NP, we did not observe large modifications of the size and the zeta potential when associated with proteins. However, PLGA NPs are spherical particles (Movva Snehalatha, 2008; Sanna et al., 2012) and it is likely that the proteins only interact with the nanoparticles' surface. Indeed, the insertion of a protein during the synthesis of PLGA NP might denature its native form (Castellanos and Griebenow, 2003; van de Weert et al., 2000). Therefore, the post-loading method is the preferred process to associate proteins to PLGA NP.

We then evaluated the protein delivery in 3 cell lines representative of the airway mucosal tissue: epithelial cells, dendritic cells and macrophages. To keep consistency, the same amount of nanocarriers was used all along the comparison. In these cell lines, all of the 5 types of nanoparticles delivered the OVA protein. However, the NPL was much more efficient in this regard than the 4 other types of nanoparticles tested. The difference appeared in the first 30 min for epithelial and dendritic cells and after only 2 h in macrophages. This implies that using NPL for protein delivery will not require an overly long exposure time of the nanocarrier with cells or tissues (Bernocchi et al., 2016; Dimier-Poisson et al., 2015; Le et al., 2018).

The kinetics of protein delivery by the 5 types of nanoparticles varied between the cell types, and especially in macrophages. In these cells, one cannot preclude that non-specific phagocytosis and

pinocytosis occurred in combination with endocytosis, leading to a constant, non-saturated protein delivery over 24 h. This is supported by the protein delivery by PLGA NP and the liposomes that were very similar to the protein endocytosis (1.5 time increase).

The efficiency of protein delivery is influenced by the endocytosis of the formulation, its adsorption to the cellular surface, as well as the amount of protein that is desorbed from the NP before reaching the cells. Since OVA was post-loaded, and due to the nature of the liposomes and PLGA NP, the OVA is associated to the surface of these nanoparticles. The desorption of OVA before these nanoparticles reach the cells cannot be precluded, but our main hypothesis remains the low cellular association (endocytosis and cellular absorption) of the PLGA NP and the liposomes (Le et al., 2018). On the contrary, the porous structure of the NPL (Le et al., 2018; Paillard et al., 2010) explains our finding that the zeta potential was not influenced by the loading of OVA, meaning protein is incorporated inside these particles. This may limit the protein desorption. However, the NPL/OVA formulation could also be attached to the cellular surface. Using quenching experiments with Trypan Blue (Bernocchi et al., 2016), only a low amount of NP appeared to be on the cellular surface. This does not exclude that some of these particles do not enter the cells, but also does not explain the significant difference of efficacy of NPL with respect to protein delivery compared to the 4 other types of nanoparticles studied here.

To our knowledge, this is the first study to compare several types of nanocarriers currently under investigation for the delivery of proteins in airways. We have previously shown that intranasal administration of a total extract of *Toxoplasma gondii* loaded into NPL afforded protection against this parasite by oral challenge in both chronical and congenital contexts (Dimier-Poisson et al., 2015; Ducournau et al., 2017), and that NPL also increased the nasal residence time of proteins (Bernocchi et al., 2016). Compared to the other nanoparticles studied here, NPL are the most endocytosed, have the longest mucosal residence time (Le et al., 2018), incorporate the greatest amount of proteins and deliver these proteins into cells the most efficiently, probably owing to their zeta potential and their porous nature. Moreover, NPL are non-toxic and suitable for *in vivo* intranasal applications (Carpentier et al., 2018). Taken together with the current study, these data underline the potential for NPL as a nanocarrier for the delivery of nasally-administered vaccines. Further studies to examine the molecular structure of NPL and the interaction between proteins and NPL using FTIR, DSC and XRD, would offer a better understanding of the mechanisms involved in NPL-protein association and protein delivery.

5. Conclusion

The development of a nasally-administered, nanoparticle-based vaccine requires nanocarriers capable of being loaded with antigens that enter the mucosal cells in order to deliver these antigens into cells. Among the 5 types of nanoparticles tested here, the cationic and porous maltodextrin-based NPL nanoparticles were the best candidate for protein loading and protein delivery. Studies should now be performed *in vivo*, taking appropriate account of the specific biological environment.

Acknowledgements

This research has received funding from the People Program (Marie Curie Actions) of the European Union Seventh Framework Program FP7/2007-2013/ under REA grant agreement no. [607690]. The authors are grateful to Michael Howsam for critically reading the manuscript and to the BICeL (campus HU) for technical support.

Conflict of interest

The authors declare no conflict of interest.

References

Azizi, A., Kumar, A., Diaz-Mitoma, F., Mestecky, J., 2010. Enhancing oral vaccine potency by targeting intestinal M cells. PLoS Pathogens 6, e1001147.
Bankvall, M., Jontell, M., Wold, A., Ostman, S., 2018. Tissue-specific differences in immune cell subsets located in the naso-oropharyngeal-associated lymphoid tissues. Scand. J. Immunol. 87, 15–27.
Batzri, S., Korn, E.D., 1973. Single bilayer liposomes prepared without sonication. Biochim. Biophys. Acta 298, 1015–1019.
Bernocchi, B., Carpentier, R., Lantier, I., Ducournau, C., Dimier-Poisson, I., Betbeder, D., 2016. Mechanisms allowing protein delivery in nasal mucosa using NPL nanoparticles. J. Control. Release 232, 42–50.
Bernocchi, B., Carpentier, R., Betbeder, D., 2017. Nasal nanovaccines. Int. J. Pharm. 530, 128–138.
Boyaka, P.N., 2017. Inducing mucosal IgA: a challenge for vaccine adjuvants and delivery systems. J. Immunol. 199, 9–16.
Carpentier, R., Platel, A., Salah, N., Nesslany, F., Betbeder, D., 2018. Porous maltodextrin-based nanoparticles: a safe delivery system for nasal vaccines. J. Nanomater (in press).
Castellanos, I.J., Griebenow, K., 2003. Improved alpha-chymotrypsin stability upon encapsulation in PLGA microspheres by solvent replacement. Pharm. Res. 20, 1873–1880.
Chang, J., Jallouli, Y., Kroubi, M., Yuan, X.B., Feng, W., Kang, C.S., Pu, P.Y., Betbeder, D., 2009. Characterization of endocytosis of transferrin-coated PLGA nanoparticles by the blood-brain barrier. Int. J. Pharm. 379, 285–292.
Clawson, C., Huang, C.T., Futalan, D., Seible, D.M., Saenz, R., Larsson, M., Ma, W., Minev, B., Zhang, F., Ozkan, M., Ozkan, C., Esener, S., Messmer, D., 2010. Delivery of a peptide via poly(D, L-lactic-co-glycolic) acid nanoparticles enhances its dendritic cell-stimulatory capacity. Nanomed. Nanotechnol. Biol. Med. 6, 651–661.
Colletier, J.P., Chaize, B., Winterhalter, M., Fournier, D., 2002. Protein encapsulation in liposomes: efficiency depends on interactions between protein and phospholipid bilayer. BMC Biotechnol. 2, 9.
Csaba, N., Garcia-Fuentes, M., Alonso, M.J., 2009. Nanoparticles for nasal vaccination. Adv. Drug Deliv. Rev. 61, 140–157.
Danhier, F., Ansorena, E., Silva, J.M., Coco, R., Le Breton, A., Preat, V., 2012. PLGA-based nanoparticles: an overview of biomedical applications. J. Control. Release 161, 505–522.
De Serrano, L.O., Burkhart, D.J., 2017. Liposomal vaccine formulations as prophylactic agents: design considerations for modern vaccines. J. Nanobiotechnol. 15, 83.
Dimier-Poisson, I., Carpentier, R., N'Guyen, T.T., Dahmani, F., Ducournau, C., Betbeder, D., 2015. Porous nanoparticles as delivery system of complex antigens for an effective vaccine against acute and chronic Toxoplasma gondii infection. Biomaterials 50, 164–175.
Diwan, M., Elamanchili, P., Lane, H., Gainer, A., Samuel, J., 2003. Biodegradable nanoparticle mediated antigen delivery to human cord blood derived dendritic cells for induction of primary T cell responses. J. Drug Target. 11, 495–507.
Dombu, C., Carpentier, R., Betbeder, D., 2012. Influence of surface charge and inner composition of nanoparticles on intracellular delivery of proteins in airway epithelial cells. Biomaterials 33, 9117–9126.
Ducournau, C., Nguyen, T.T., Carpentier, R., Lantier, I., Germon, S., Precausta, F., Pisella, P.J., Leroux, H., Van Langendonck, N., Betbeder, D., Dimier-Poisson, I., 2017. Synthetic parasites: a successful mucosal nanoparticle vaccine against Toxoplasma congenital infection in mice. Future Microbiol. 12, 393–405.
Fujkuyama, Y., Tokuhara, D., Kataoka, K., Gilbert, R.S., McGhee, J.R., Yuki, Y., Kiyono, H., Fujihashi, K., 2012. Novel vaccine development strategies for inducing mucosal immunity. Expert Rev. Vac. 11, 367–379.
Gradauer, K., Vonach, C., Leitinger, G., Kolb, D., Frohlich, E., Roblegg, E., Bernkop-Schnurch, A., Prassl, R., 2012. Chemical coupling of thiolated chitosan to preformed liposomes improves mucoadhesive properties. Int. J. Nanomed. 7, 2523–2534.
Jallouli, Y., Paillard, A., Chang, J., Sevin, E., Betbeder, D., 2007. Influence of surface charge and inner composition of porous nanoparticles to cross blood-brain barrier in vitro. Int. J. Pharm. 344, 103–109.
Juliusson, S., Bachert, C., Klementsson, H., Karlsson, G., Pipkorn, U., 1991. Macrophages on the nasal mucosal surface in provoked and naturally occurring allergic rhinitis. Acta Otolaryngol. 111, 946–953.
Kurakula, K., Hamers, A.A., van Loenen, P., de Vries, C.J., 2015. 6-Mercaptopurine reduces cytokine and Muc5ac expression involving inhibition of NFkappaB activation in airway epithelial cells. Respir. Res. 16, 73.
Le Broc-Ryckewaert, D., Carpentier, R., Lipka, E., Daher, S., Vaccher, C., Betbeder, D., Furman, C., 2013. Development of innovative paclitaxel-loaded small PLGA nanoparticles: study of their antiproliferative activity and their molecular interactions on prostatic cancer cells. Int. J. Pharm. 454, 712–719.
Le, M.Q., Carpentier, R., Lantier, I., Ducournau, C., Dimier-Poisson, I., Betbeder, D., 2018. Residence time and uptake of porous and cationic maltodextrin-based nanoparticles in the nasal mucosa: comparison with anionic and cationic nanoparticles. Int. J. Pharm. 550, 316–324.
Lee, Y.R., Lee, Y.H., Im, S.A., Kim, K., Lee, C.K., 2011. Formulation and characterization of antigen-loaded PLGA nanoparticles for efficient cross-priming of the antigen. Immune Netw. 11, 163–168.
Marasini, N., Skwarczynski, M., Toth, I., 2017. Intranasal delivery of nanoparticle-based vaccines. Therap. Deliv. 8, 151–167.
Movva Snehalatha, K.V., Saha, Ranendra, 2008. Etoposide-loaded PLGA and PCL nanoparticles I: preparation and effect of formulation variables. Drug Deliv. 15, 267–275.
Ogra, P.L., Faden, H., Welliver, R.C., 2001. Vaccination strategies for mucosal immune responses. Clin. Microbiol. Rev. 14, 430–445.

Oh, N., Park, J.H., 2014. Endocytosis and exocytosis of nanoparticles in mammalian cells. Int. J. Nanomed. 9 (Suppl. 1), 51–63.
Pachioni-Vasconcelos Jde, A., Lopes, A.M., Apolinario, A.C., Valenzuela-Oses, J.K., Costa, J.S., Nascimento Lde, O., Pessoa, A., Barbosa, L.R., Rangel-Yagui Cde, O., 2016. Nanostructures for protein drug delivery. Biomater. Sci. 4, 205–218.
Paillard, A., Passirani, C., Saulnier, P., Kroubi, M., Garcion, E., Benoit, J.P., Betbeder, D., 2010. Positively-charged, porous, polysaccharide nanoparticles loaded with anionic molecules behave as 'stealth' cationic nanocarriers. Pharm. Res. 27, 126–133.
Patil, Y.P., Jadhav, S., 2014. Novel methods for liposome preparation. Chem. Phys. Lipids 177, 8–18.
Prasad, S., Cody, V., Saucier-Sawyer, J.K., Saltzman, W.M., Sasaki, C.T., Edelson, R.L., Birchall, M.A., Hanlon, D.J., 2011. Polymer nanoparticles containing tumor lysates as antigen delivery vehicles for dendritic cell-based antitumor immunotherapy. Nanomed. Nanotechnol. Biol. Med. 7, 1–10.
Rivera, A., Siracusa, M.C., Yap, G.S., Gause, W.C., 2016. Innate cell communication kick-starts pathogen-specific immunity. Nat. Immunol. 17, 356–363.
Ruiz, S., Beauvillain, C., Mevelec, M.N., Roingeard, P., Breton, P., Bout, D., Dimier-Poisson, I., 2005. A novel CD4-CD8alpha + CD205 + CD11b-murine spleen dendritic cell line: establishment, characterization and functional analysis in a model of vaccination to toxoplasmosis. Cell. Microbiol. 7, 1659–1671.
Sanna, V., Roggio, A.M., Siliani, S., Piccinini, M., Marceddu, S., Mariani, A., Sechi, M., 2012. Development of novel cationic chitosan-and anionic alginate-coated poly(D, L-lactide-co-glycolide) nanoparticles for controlled release and light protection of resveratrol. Int. J. Nanomed. 7, 5501–5516.
Solbrig, C.M., Saucier-Sawyer, J.K., Cody, V., Saltzman, W.M., Hanlon, D.J., 2007. Polymer nanoparticles for immunotherapy from encapsulated tumor-associated antigens and whole tumor cells. Mol. Pharm. 4, 47–57.
Thomas, C., Rawat, A., Hope-Weeks, L., Ahsan, F., 2011. Aerosolized PLA and PLGA nanoparticles enhance humoral, mucosal and cytokine responses to hepatitis B vaccine. Mol. Pharm. 8, 405–415.
Torchilin, V.P., 2005. Recent advances with liposomes as pharmaceutical carriers. Nat. Rev. Drug Discov. 4, 145–160.
van de Weert, M., Hennink, W.E., Jiskoot, W., 2000. Protein instability in poly(lactic-co-glycolic acid) microparticles. Pharm. Res. 17, 1159–1167.
Watson, D.S., Endsley, A.N., Huang, L., 2012. Design considerations for liposomal vaccines: influence of formulation parameters on antibody and cell-mediated immune responses to liposome associated antigens. Vaccine 30, 2256–2272.
Weitnauer, M., Mijosek, V., Dalpke, A.H., 2016. Control of local immunity by airway epithelial cells. Mucosal Immunol. 9, 287–298.
Xu, X., Khan, M.A., Burgess, D.J., 2011. A quality by design (QbD) case study on liposomes containing hydrophilic API: I. Formulation, processing design and risk assessment. Int. J. Pharm. 419, 52–59.
Yang, Y.W., Luo, W.H., 2017. Recruitment of bone marrow CD11b(+)Gr-1(+) cells by polymeric nanoparticles for antigen cross-presentation. Sci. Rep. 7, 44691.
Zaman, M., Chandrudu, S., Toth, I., 2013. Strategies for intranasal delivery of vaccines. Drug Deliv. Transl. Res. 3, 100–109.
Zhao, L., Seth, A., Wibowo, N., Zhao, C.X., Mitter, N., Yu, C., Middelberg, A.P., 2014. Nanoparticle vaccines. Vaccine 32, 327–337.